

Towards Efficient Entropic Recycling by Mastering Ring-Chain Kinetics

Jeffrey C. Foster,^{1,*} Isaiah T. Dishner¹, Joshua T. Damron¹, Vilmos Kertesz², Ilja Popovs¹, and Tomonori Saito¹

¹Chemical Sciences Division, Oak Ridge National Laboratory, Oak Ridge, Tennessee 37831, United States

²Biosciences Division, Oak Ridge National Laboratory, Oak Ridge, Tennessee 37831, United States

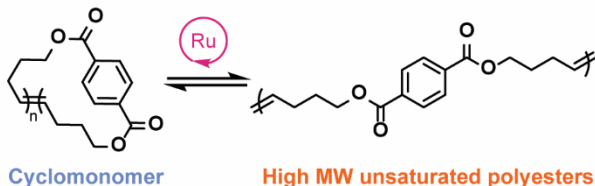
Corresponding author: fosterjc@ornl.gov (J.C.F)

Keywords: Polymerization, polymers, macrocycles

This manuscript has been authored by UT-Battelle LLC under contract DE-AC05-00OR22725 with the U.S. Department of Energy (DOE). The U.S. government retains, and the publisher, by accepting the article for publication, acknowledges that the U.S. government retains a nonexclusive, paid-up, irrevocable, worldwide license to publish or reproduce the published form of this manuscript, or allow others to do so, for U.S. government purposes. DOE will provide public access to these results of federally sponsored research in accordance with the DOE Public Access Plan (<http://energy.gov/downloads/doe-public-access-plan>).

For Table of Contents use only

Catalyst-controlled Entropic Synthesis and Recycling



- Chain-growth • Energy efficient • 0.1 M Cyclodepolymerization

Abstract

Traditional chemical recycling approaches for condensation polymers suffer compounding energy losses and CO₂ emissions across multiple polymerization and depolymerization cycles. Entropic recycling can address these energy losses by entrapping free energy within the deconstruction products. Entropic recycling involves depolymerization to macrocyclic monomers, but such processes have not been feasible due to the high dilutions typically required to generate macrocyclic compounds. Here, we leverage selective catalysis to allow entropic recycling at

concentrations 20-2000X higher than typical for macrocyclization reactions. We find that Ru-based olefin metathesis catalysts containing bulky iodine ligands significantly bias the ring-chain kinetic product distribution during ring-closing metathesis (RCM) towards the formation of oligomeric cycloalkenes. Further improvements in reaction concentration and macrocycle yield are obtained by using high catalyst loadings and by pre-disposing the alkene substrates to undergo favorable macrocyclization. These RCM optimizations translated effectively to cyclodepolymerization (CDP) of an olefin-containing polymer, with RCM and CDP affording similar macrocycle product distributions under identical reaction conditions. Macrocycle polymerization by entropy-driven ring-opening metathesis (ED-ROMP) provides much higher molecular weight polymers than condensation polymerization of linear analogues, reducing the time to achieve high molecular weight from hours to minutes, and enabling polymerization at room temperature. Our findings re-emphasize the importance of energy consumption during a polymer's lifecycle and provide a framework for the design of efficient entropic recycling systems.

Introduction

The rapid growth of the plastics manufacturing industry in combination with the lack of sustainable technologies to manage waste plastics at their end-of-life has created a global challenge of establishing plastics circularity. Only a fraction of used plastic material is currently recycled,¹ driving its accumulation in the environment and wasting the feedstock resources and energy consumed for its production. Chemical recycling approaches, which typically generate small molecule building blocks that can be used to resynthesize the parent polymers, have laid the foundation for a circular plastics economy.²⁻⁴ However, such approaches still lack energy efficiency and, while effective for reducing plastic waste accumulation, generate significant

greenhouse gas (GHG) emissions that are compounded across numerous polymerization/deconstruction cycles.⁵

Condensation (or step-growth) polymers such as polyethylene terephthalate (PET) comprise a large proportion of the plastics market.⁶ PET is synthesized via a weakly exothermic condensation reaction that requires significant heating (typically at 280 °C) to achieve reasonable reaction rates, inhibit crystallization of the growing polymer, and drive off condensation byproducts (Figure 1).⁷ Its deconstruction, for example by glycolysis, requires equally high thermal energy and sacrifices the moderate thermodynamic energy gained during polymerization. Tradeoffs between energy efficiency and feedstock recovery are shared across most circular condensation polymer systems, notable for polyesters and polyamides and exaggerated for polyurethanes and polycarbonates due to CO₂ loss during deconstruction.

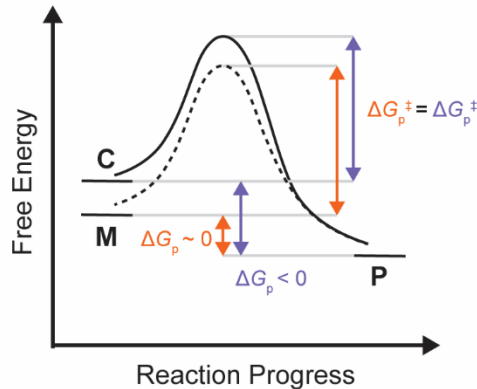
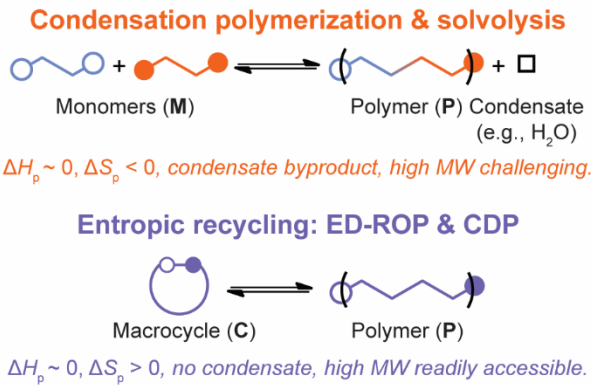


Figure 1. Thermodynamic comparison of selected polymer synthesis and deconstruction pathways.

Polymer deconstruction by cyclodepolymerization (CDP) and re-synthesis by entropy-driven ring-opening polymerization (ED-ROP) has emerged as a promising alternative paradigm for circularity (so called “entropic recycling”).⁸ Entropic recycling improves energy efficiency by entrapping a portion of the thermal energy invested during depolymerization into free energy via the decreased degrees of rotational and vibrational motion accessible to macrocycles compared with linear analogues (Figure 1). This entrapped free energy, stored within macrocycles as conformational entropy, enables re-polymerization via a chain-growth mechanism that precludes condensate formation and provides a driving force to access polymers with higher molecular weights (MWs) compared with traditional condensation polymerization.⁹⁻¹¹ Further, ED-ROP enables precise MW targeting through simple tuning of initial reaction conditions.

Circular CDP/ED-ROP systems have been developed using a broad variety of macrocyclic monomers including cyclic esters,¹²⁻¹⁸ sulfur-containing compounds,¹⁹⁻²¹ and many other functional motifs.²²⁻²⁵ Despite their potential, these successful demonstrations have reinforced the limitations of entropic recycling that derive from the nature of ring-chain equilibrium processes: high dilution (e.g., 0.05-5 mM substrate concentration) and near quantitative conversion are required to favor the formation of macrocycles over linear oligomeric species during CDP.²⁶ To enhance the feasibility of entropic recycling, CDP (or ring-closing macrocyclization reactions to make the initial monomers) must be facile at high concentration and produce high yields of macrocycles that are readily separable from linear impurities. Doing so requires control over ring-chain equilibria to be established, for example through biasing the kinetic product distribution towards the formation of macrocycles.²⁷

In this contribution, we explore the impact of selective catalysis on ring-closing macrocyclization and thus CDP. Using a PET-adjacent unsaturated polyester system reported in our previous work and olefin metathesis chemistry,²⁸ we reveal that the ring-chain kinetic product distribution can be significantly biased in favor of macrocycle formation by using selective Ru-based catalysts and tuning their concentration, with high catalyst loadings providing high yields of macrocycles at substrate concentrations up to 20 mM. This catalyst concentration effect was found to originate an enhanced tendency for cyclization relative to chain elongation. Tailoring substrate structure, combined with high catalyst loading, enabled the concentration of the macrocyclizations to be further increased to 100 mM while maintaining good yields and facilitating simple macrocycle purification. These comparative substrate experiments highlighted the inherent tradeoffs between cyclization tendency, polymerizability, and the thermal properties of the resultant materials. High selectivity was maintained when these principles were applied for CDP. Overall, this investigation provides a framework to reimagine polymer circularity and rationally design future polymer systems to address all aspects of circularity from energy efficiency to reduced environmental accumulation and beyond.

Results and Discussion

To highlight the potential of entropic recycling, we first compared condensation polymerization to ED-ROP using an olefin metathesis model system (Figure 2A). In our previous report, acyclic diene metathesis (ADMET) polymerization was successfully demonstrated for α,ω -dialkenyl terephthalate monomers derived from PET waste.²⁸ While this strategy provided unsaturated polyesters with good recyclability, the ADMET polymerizations took several days under heating and dynamic vacuum to produce polymers with sufficient molecular weight MW for desirable thermomechanical performance. In the present work, ADMET polymerization was carried out

using di(pent-4-en-1-yl) terephthalate (**DPT**) (Figures S1-S2) using **GI** (Scheme 1) in 1,2,4-trichlorobenzene at 60 °C under dynamic vacuum for 16 h (Figure S3). Similar to our previous report, poly(**DPT**) was obtained with a low number average MW, M_n , of 9.0 kg mol⁻¹ and a broad dispersity, $D = 3.44$ (Figure 2B). **DPT** cyclodimer (**cDPT**, $n = 2$) was prepared for comparison via ring-closing metathesis (RCM) of **DPT** mediated by **GII** under dilute conditions (5 mM substrate concentration) and subsequent chromatographic purification (Figures S4-S6). Its polymerization by entropy-driven ring-opening metathesis polymerization (ED-ROMP) using **GIII** achieved a significantly higher M_n of 60.2 kg mol⁻¹ in just 1 h at room temperature and ambient pressure (Figure 2B and Figure S7). Further, ED-ROMP of **cDPT** enabled easy targeting of M_n from ca. 20-60 kg mol⁻¹ by simply changing the amount of catalyst used (Figure 2C and 2D, Table S1) or the monomer concentration (Figures S8-S9, Table S1), consistent with related reports.^{12, 14, 24}

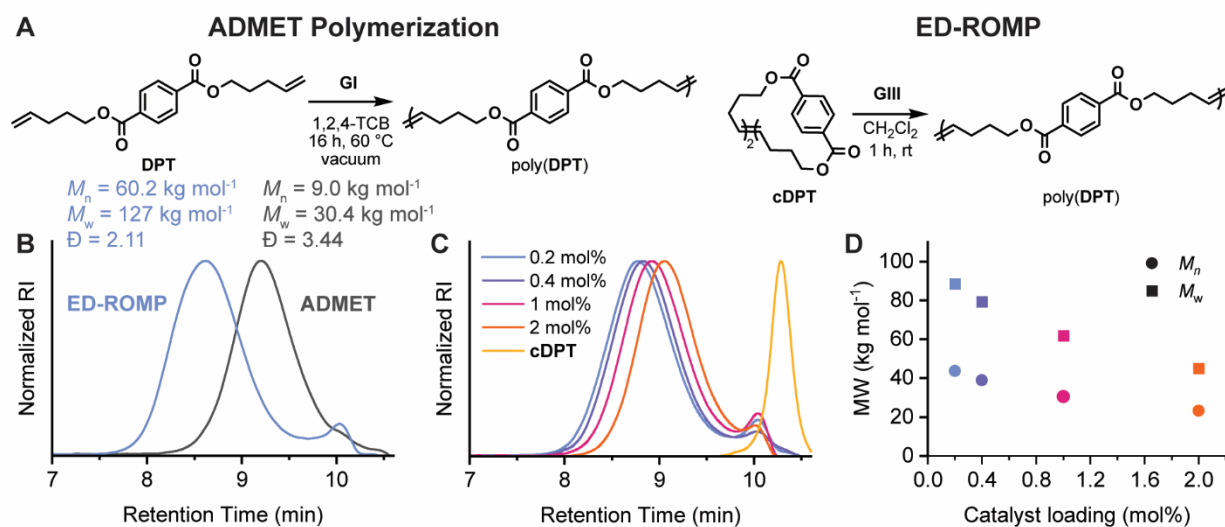
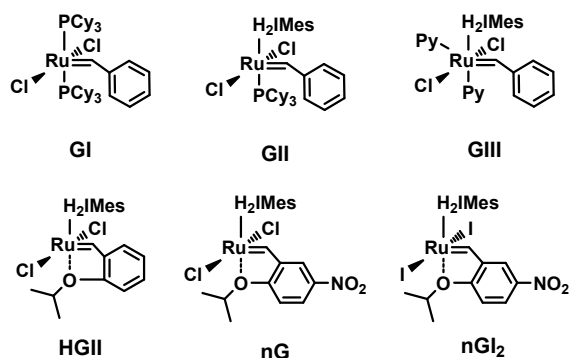


Figure 2. A) Conditions used for ADMET polymerization of **DPT** and ED-ROMP of **cDPT**. B) Normalized SEC traces of polymers obtained via ADMET polymerization of **DPT** or ED-ROMP of **cDPT**. C) Normalized SEC traces of poly(**DHT**) produced by ED-ROMP using different catalyst concentrations. D) Plot of M_n and M_w vs catalyst loading calculated from the SEC data shown in C.

Despite the improvements in energy efficiency and MW control afforded by ED-ROMP of **cDPT** compared with ADMET of its linear analogue **DPT**, the synthesis of **cDPT** required high dilution, (5 mM), a long reaction time (16 h), and complicated chromatographic purification. Indeed, RCM of **DPT** produced a distribution of cyclic products including the cyclodimer and various higher cyclooligomers (Figure S10), resulting in only a moderate isolated yield of **cDPT** (38%). As such, we sought to compare various Ru-based olefin metathesis catalysts under a variety of reaction conditions with the goals of increasing **cDPT** yields, increasing substrate concentrations, and decreasing reaction times.

To identify high-performing Ru catalysts for macrocyclization reactions, several complexes were screened under otherwise identical conditions. The screening panel included the traditional **GII** complex, **HGII** and **nG**, both of which are known to be good catalysts for RCM, and **nGI₂**, a congener of **nG** containing bulky iodine ligands (Scheme 1).²⁹ Screening reactions were carried out with 5 mM **DPT** in toluene at 80 °C in sealed vials (no active ethylene removal) to compare **RCM** conversions under challenging conditions. As shown in Table S2, **nGI₂** significantly outperformed the other catalysts after 1 h in terms of conversion. Intriguingly, **nGI₂** provided higher conversions than its congener **nG** in a range of solvents (Table S3), providing some evidence for its enhanced stability and/or its selectivity for reactions involving terminal alkenes.²⁹ Further evidence of selectivity was observed through the slow ROMP of cyclooctadiene (COD) by **nGI₂** relative to **nG** (Figure S11), consistent with observations on related catalysts containing iodine ligands.³⁰ The combination of high reactivity and high selectivity motivated us to further explore **nGI₂** for macrocyclization.

Scheme 1. Catalysts used in this study.



We next evaluated the performance of **nGI₂** for RCM of **DPT** at different substrate concentrations and catalyst loadings (Figure 3A). This set of reactions were carried out for 1 h in refluxing CH₂Cl₂ to promote active removal of ethylene, a byproduct of olefin metathesis reactions between terminal alkenes (Scheme 2). Increased catalyst loadings generally increased RCM conversions (Figure 3B), while the effect of substrate concentration was more complex. Conversions appeared to increase with increasing substrate concentration up to 100 mM, after which they decreased. This observation implicated a concentration-dependent change in mechanism that we attributed to suppression of intramolecular cyclization at high substrate concentration ($k_2 > k_2$, Scheme 2). Further insight was gained by comparing experimentally measured M_n values for the various RCM reactions obtained from SEC against theoretical values calculated based on conversions using the Carothers equation, noting that each equivalent of Ru catalyst introduced an additional styrenic polymer chain end

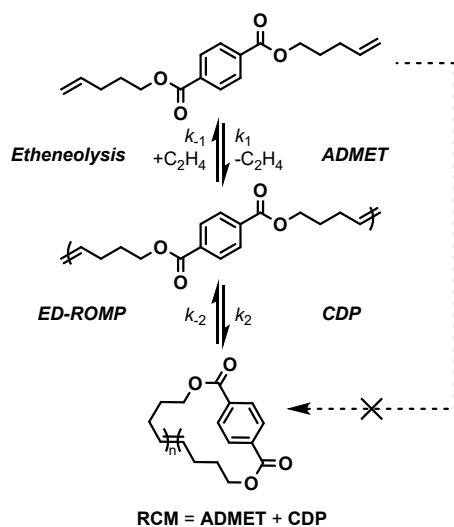
$$M_{n,theo} = M_0 \frac{1+r}{1+r-2rp} \quad (1)$$

$$r = \frac{N_A}{N_A + 2N_{Ru}} \quad (2)$$

where M_0 represents the MW of the repeating unit, r the stoichiometric ratio of reactants, p is conversion, N_A is the relative fraction of bifunctional monomers, and N_{Ru} is the relative fraction

of Ru catalyst. These theoretical values represent M_n s that would be expected from chain extension via intermolecular cross-metathesis in the absence of cyclization. As shown in Figure 3B, experimentally measured M_n values deviated significantly from expectations at high catalyst loadings. Further, these deviations were maximized at the highest conversions. Taken together, these data suggested a kinetic bias of **nGI**₂ towards intramolecular cyclization at ≤ 100 mM substrate ($k_2 > k_{-2}$, Scheme 2). We note that the formation of macrocycles was strongly indicated when M_n was low at high conversion (i.e., self-dilution behavior^{31, 32}) and this indicator was further exploited in subsequent kinetic analyses.

Scheme 2. Overview of olefin metathesis transformations relevant to this work.



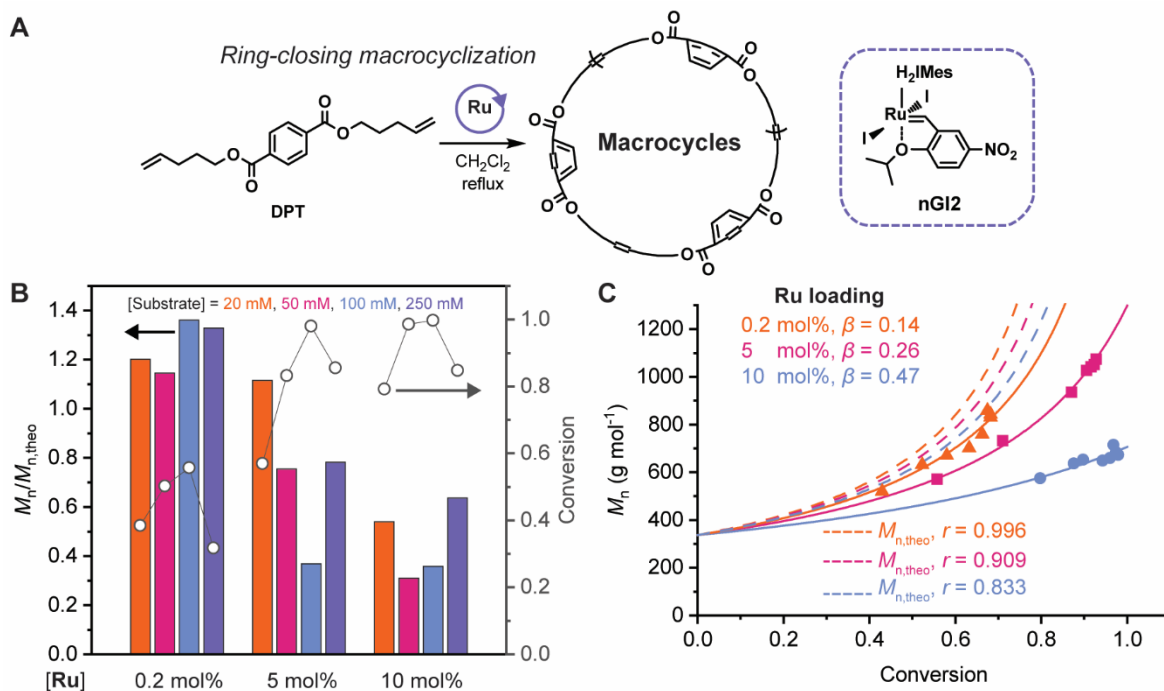


Figure 3. A) Exploration of RCM of **DPT** using **nGI₂**. B) Visualization of experimentally measured fraction of theoretical M_n and conversion for RCM reactions at different substrate and catalyst concentrations. C) Plot of M_n vs conversion for RCMs with different catalyst loadings. The data are fit with Equation 3 (below). The dashed lines represent theoretical molecular weights based on initial reaction stoichiometries calculated using Equations 1 and 2.

The kinetic behavior of RCM of **DPT** by **nGI₂** was investigated at 100 mM, where optimal conversions and low M_n s were obtained in the previous experiments, and with different catalyst loadings. Aliquots of RCMs with 0.2, 5, and 10 mol% **nGI₂** were sampled at various intervals and quenched by adding ethyl vinyl ether. Conversion data for the RCMs were best described by second-order kinetic plotting (Figure S12), with increased catalyst loading affording faster RCM approaching quantitative conversions with 10 mol% **nGI₂** within 1 h. Plotting M_n against conversion for these RCMs revealed a significant deviation from Carothers' description of intermolecular chain elongation (Figure 3C), further suggesting that intramolecular cyclization

was occurring to a significant degree even at a substrate concentration that was 20-2000X higher than is typical for RCM.³³ Instead, the kinetic data in Figure 3C were well-described by a modified Carothers equation that accounts for intramolecular ring-chain and ring-ring equilibria³⁴

$$M_n = M_0 \frac{1}{[1 - p(1 - \beta)]} \quad (3)$$

where β represents a kinetic or thermodynamic tendency for cyclization. In this treatment, $\beta = 0$ corresponds with no cyclization and $\beta = 1$ with the complete conversion of substrate to macrocycles in the absence of intermolecular elongation. Intriguingly, cyclization tendency increased with increased catalyst loading (i.e., $k_2 \propto [Ru]$, Scheme 2), consistent with a higher-order concentration dependence for intramolecular reaction rates when using **nGI₂** compared with intermolecular reactions. This concept was further corroborated by the observed non-linear relationship between observed rate constants, k_{obs} , and catalyst concentration for these experiments (Figure S13). Visualizing these data in view of the deviation of M_n from expected values (Figure S14), the formation of small macrocycles was also apparent as a consistent increase in deviation with increasing conversion. Based on these observations and on the law of self-dilution, we anticipate that the yield of small macrocycles should be maximized at increasing reaction times approaching $p = 1$.

To further maximize the fraction of small macrocycles produced by RCM of **DPT** with **nGI₂**, additional experiments were conducted by varying substrate concentration (Figure 4A1). These RCMs were allowed to react for 4 h to target near quantitative conversions. At 100 mM **DPT**, RCM produced a very broad distribution of products as evidenced by the multimodal molecular weight distribution (MWD) obtained via SEC. The fraction of higher MW species was reduced at 50 mM **DPT** and all but eliminated at 20 mM **DPT**, enabling the cyclodimer to be easily isolated

via silica gel chromatography in moderate yield (Figure 4B1 and Table S4). **cDPT** cyclodimer ($n = 2$) prepared by **nGI**₂ was readily polymerized by ED-ROMP using **GIII** at 1 M in CH₂Cl₂ at room temperature, providing poly(**DPT**) with significantly higher M_n than ADMET polymerization of linear **DPT** (Figure 4C1 and Table S5).

We then explored the influence of aromatic ring substitution on RCM equilibrium. We hypothesized that meta- or ortho-substituted analogues of **DPT** might bias ring-closing over oligomerization due to preorganization of their α and ω terminal alkenes. Towards this end, **DPI** (Figures S15-S16) and **DPP** (Figures S17-S18) were synthesized via esterification of 5-penten-1-ol and isophthalic acid or phthalic acid, respectively. RCM of **DPI** using 10 mol% **nGI**₂ produced a distribution of cyclic products comprising a much larger proportion of small macrocycles compared with **DPT**, enabling moderate isolated yields of cyclooligomers at 50 mM substrate (Figures 4A2 and 4B2, Table S4). For this system, cyclodimer **cDPI** was isolated as the major RCM product, similar to the reactions with **DPT** (Figures S19-S21). The isolated cyclodimer, **cDPI**, was also amenable to ED-ROMP and produced poly(**DPI**) (Figure 4C2, Table S5, and Figure S23). As with the terephthalate system, ED-ROMP of **cDPI** outperformed its analogous ADMET polymerization (Figure S22) in terms of achievable MW and energy efficiency, striking a good compromise between cyclization concentration, yield, and polymerizability. When **DPP** was used as the substrate for RCM, cyclomonomer ($n = 1$) was obtained in high yield even up to 100 mM substrate concentration (Figure 4A3 and 4B3, Table S4, and Figures S24-S26). However, despite its privileged cyclization behavior, ED-ROMP of cyclomonomer **cDPP** did not produce detectable quantities of polymer despite multiple attempts at different concentrations (1-2 M) or different reaction times (1-4 h). We note that ADMET polymerization of **DPP** was possible (ca. 5X higher monomer concentration compared with ED-ROMP), suggesting that a pathway may

exist for its ED-ROMP if sufficiently high monomer concentrations could be achieved (Figure 4C3, Table S5, and Figure S27). Overall, the terephthalate and isophthalate substrates gave cyclodimers as the major product of RCM, with **cDPT** providing higher MW polymers by ED-ROMP but **cDPI** enabling RCM at higher concentration. In contrast, the phthalate derivative **DPP** was cyclized almost quantitatively to **cDPP** even at 100 mM; however, **cDPP** was inactive for ED-ROMP. Tradeoffs in material properties must also be considered in addition to cyclization and polymerization behavior. Poly(**PDT**) was semi-crystalline as determined by differential scanning calorimetry (DSC), with a melting temperature, T_m , of 78.8 °C and a glass transition temperature, T_g , of -13.1 °C (Figure S28). In contrast, poly(**DPI**) and poly(**DPP**) were amorphous, with T_g 's of -17.3 °C and -21.6 °C, respectively (Figure S28). These data reinforce the fine sensitivity of macrocyclization reactions to substrate structure and highlight how the combination of a selective catalyst, a high catalyst concentration, and a readily cyclizable substrate can be leveraged to finely tune ring-chain equilibria in favor of either macrocycles or high MW polymers.

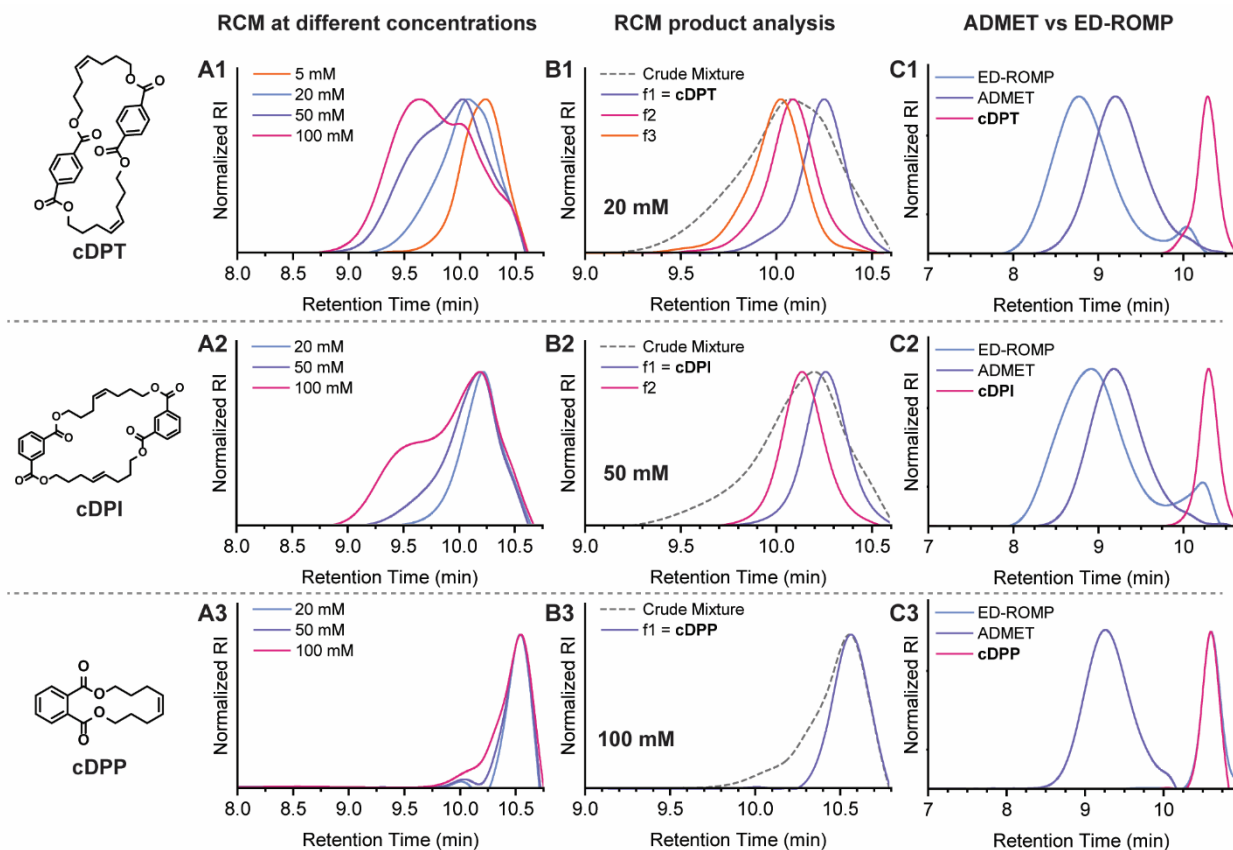


Figure 4. From left to right: normalized SEC traces of RCMs using 10 mol% \mathbf{nGI}_2 at different monomer concentrations (column A), normalized SEC traces of the crude RCM reaction mixture at 20, 50, or 100 mM and those of the various macrocycles isolated from these mixtures by chromatography (column B), and normalized SEC comparison of ADMET using linear monomers against ED-ROMP using cyclomonomers for **cDPT** (1), **cDPI** (2), and **cDPP** (3) (column C). The legends in column B represent the various pure fractions of macrocycles isolated via silica gel chromatography.

Finally, to evaluate the pertinency of kinetic control in entropic recycling, we sought to compare the preparation of cyclodimer **cDPT** by different pathways: (1) RCM of **DPT** (detailed above); and (2) CDP of poly(**DPT**) (Figure 5A). CDP was conducted using poly(**DPT**) and 10 mol% \mathbf{nGI}_2 in refluxing CH_2Cl_2 for 4 h. Substrate concentrations of 5 and 20 mM (relative to backbone repeat

units) were chosen to directly compare the outcomes of these experiments to the data above. As shown in Figure 5B, RCM of **DPT** and CDP of poly(**DPT**) afforded remarkably similar kinetic product distributions as judged by SEC. Minor differences were apparent for the experiments conducted at 20 mM substrate concentration, with CDP producing a relatively narrower MWD. More striking was the total absence of terminal alkenes in the crude ^1H NMR spectrum of this reaction mixture, signifying the complete conversion of the initial alkenyl endgroups of poly(**DPT**) into internal alkenes via backbiting (Table S6). Macrocycle synthesis by RCM has been shown to progress through an enchainment *then* backbiting pathway.³⁵ By using poly(**DPT**) as a substrate instead of **DPT**, the macrocyclization reaction effectively bypasses the elongation step and begins at a higher initial functional group conversion, thus achieving a theoretically higher ultimate conversion in the same timeframe. The data shown in Figure 5B and Table S6 demonstrate that RCM serves as a useful platform to optimize kinetic control over the ring-chain product distribution and that this optimization translates readily to CDP.

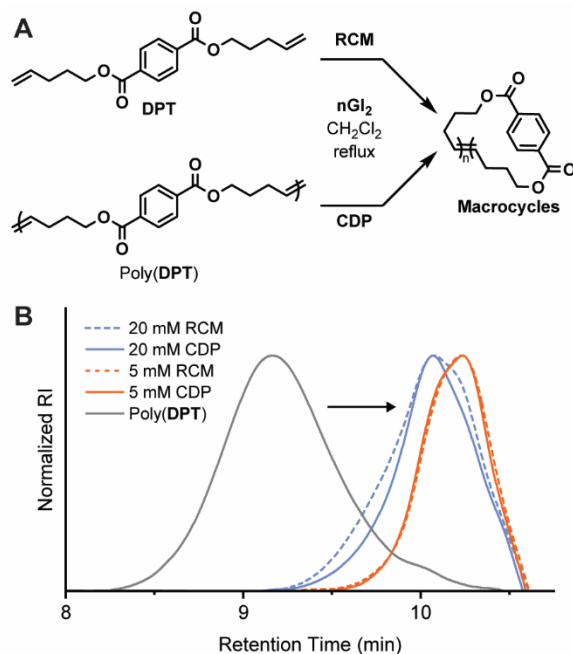


Figure 5. A) Comparison of synthesis of macrocycles via RCM using **DPT** and by CDP starting from poly(**DPT**) under otherwise identical reaction conditions. B) Normalized SEC traces of the starting poly(**DPT**) and the crude reaction mixtures following RCM or CDP at different concentrations.

Conclusions

In summary, we showed that selective catalysts can be exploited to bias ring-chain kinetic product distributions during macrocyclization reactions. Specifically, the Ru-based olefin metathesis catalyst **nGI**₂ exhibited extraordinary selectivity for terminal olefins, enabling high conversion of bis-alkenyl compounds to macrocycles at substrate concentrations up to 100 mM. This selectivity was observed to depend strongly on catalyst loading, further re-enforcing the potential of catalysis in manipulating outcomes in reactions via kinetic control. Further, catalyst selectivity was maintained across different reaction pathways, with RCM and CDP affording similar reaction outcomes. We envision that continued effort in catalyst design will ultimately enable CDP reactions to be conducted at industrially feasible concentrations, paving the way toward a polymer economy based on entropic, rather than enthalpic, polymerization and depolymerization. Entropic recycling not only addresses the accumulation of plastic waste but also significantly reduces the energy expenditures, and associated CO₂ emissions, of plastics production and recycling.

Supporting Information

The Supporting Information is available free of charge at XXX.

- Experimental methods and supplementary experimental and characterization data.

Acknowledgements

This research was supported by the US Department of Energy, Office of Science, Basic Energy Sciences, Materials Sciences and Engineering Division.

References

1. Plastics: Material-Specific Data. <https://www.epa.gov/facts-and-figures-about-materials-waste-and-recycling/plastics-material-specific-data>.
2. Zheng, J.; Arifuzzaman, M.; Tang, X.; Chen, X. C.; Saito, T., Recent development of end-of-life strategies for plastic in industry and academia: bridging their gap for future deployment. *Mater. Horiz.* **2023**, *10* (5), 1608-1624.
3. Coates, G. W.; Getzler, Y. D. Y. L., Chemical recycling to monomer for an ideal, circular polymer economy. *Nat. Rev. Mater.* **2020**, *5* (7), 501-516.
4. Schade, A.; Melzer, M.; Zimmermann, S.; Schwarz, T.; Stoewe, K.; Kuhn, H., Plastic Waste Recycling—A Chemical Recycling Perspective. *ACS Sus. Chem. & Eng.* **2024**, *12* (33), 12270-12288.
5. Bell, L. Chemical recycling: a dangerous deception. Beyond Plastics and International Pollutants Elimination Network (IPEN), October 2023.
6. Nicholson, S. R.; Rorrer, N. A.; Carpenter, A. C.; Beckham, G. T., Manufacturing energy and greenhouse gas emissions associated with plastics consumption. *Joule* **2021**, *5* (3), 673-686.
7. Zope, V. S.; Mishra, S., Kinetics of neutral hydrolytic depolymerization of PET (polyethylene terephthalate) waste at higher temperature and autogenous pressures. *J. Appl. Poly. Sci.* **2008**, *110* (4), 2179-2183.
8. Hodge, P., Recycling of condensation polymers via ring–chain equilibria. *Poly. Adv. Tech.* **2015**, *26* (7), 797-803.

9. Pearce, A. K.; Foster, J. C.; O'Reilly, R. K., Recent developments in entropy-driven ring-opening metathesis polymerization: Mechanistic considerations, unique functionality, and sequence control. *J. Poly. Sci. A* **2019**, *57* (15), 1621-1634.
10. Strandman, S.; Gautrot, J. E.; Zhu, X. X., Recent advances in entropy-driven ring-opening polymerizations. *Polym. Chem.* **2011**, *2* (4), 791-799.
11. Xue, Z.; Mayer, M. F., Entropy-driven ring-opening olefin metathesis polymerizations of macrocycles. *Soft Matter* **2009**, *5* (23), 4600-4611.
12. Nowalk, J. A.; Fang, C.; Short, A. L.; Weiss, R. M.; Swisher, J. H.; Liu, P.; Meyer, T. Y., Sequence-Controlled Polymers Through Entropy-Driven Ring-Opening Metathesis Polymerization: Theory, Molecular Weight Control, and Monomer Design. *J. Am. Chem. Soc.* **2019**, *141* (14), 5741-5752.
13. Witt, T.; Häußler, M.; Mecking, S., No Strain, No Gain? Enzymatic Ring-Opening Polymerization of Strainless Aliphatic Macrolactones. *Macromol. Rapid. Commun.* **2017**, *38* (4), 1600638.
14. Ogawa, R.; Hillmyer, M. A., High molar mass poly(ricinoleic acid) via entropy-driven ring-opening metathesis polymerization. *Polym. Chem.* **2021**, *12* (15), 2253-2257.
15. Rosenboom, J.-G.; Hohl, D. K.; Fleckenstein, P.; Storti, G.; Morbidelli, M., Bottle-grade polyethylene furanoate from ring-opening polymerisation of cyclic oligomers. *Nat. Commun.* **2018**, *9* (1), 2701.
16. Flores, I.; Martínez de Ilarduya, A.; Sardon, H.; Müller, A. J.; Muñoz-Guerra, S., Synthesis of Aromatic–Aliphatic Polyesters by Enzymatic Ring Opening Polymerization of Cyclic Oligoesters and their Cyclodepolymerization for a Circular Economy. *ACS Appl. Polym. Mater.* **2019**, *1* (3), 321-325.

17. Deng, L.-L.; Guo, L.-X.; Lin, B.-P.; Zhang, X.-Q.; Sun, Y.; Yang, H., An entropy-driven ring-opening metathesis polymerization approach towards main-chain liquid crystalline polymers. *Polym. Chem.* **2016**, *7* (33), 5265-5272.
18. Gautrot, J. E.; Zhu, X. X., Shape Memory Polymers Based on Naturally-Occurring Bile Acids. *Macromolecules* **2009**, *42* (19), 7324-7331.
19. Kariyawasam, L. S.; Highmoore, J. F.; Yang, Y., Chemically Recyclable Dithioacetal Polymers via Reversible Entropy-Driven Ring-Opening Polymerization. *Angew. Chemie. Int. Ed.* **2023**, *62* (26), e202303039.
20. Behrendt, F. N.; Schlaad, H., Entropy-Driven Ring-Opening Disulfide Metathesis Polymerization for the Synthesis of Functional Poly(disulfide)s. *Macromol. Rapid. Commun.* **2018**, *39* (6), 1700735.
21. Behrendt, F. N.; Hess, A.; Lehmann, M.; Schmidt, B.; Schlaad, H., Polymerization of cystine-derived monomers. *Polym. Chem.* **2019**, *10* (13), 1636-1641.
22. Yu, Z.; Wang, M.; Chen, X.-M.; Huang, S.; Yang, H., Ring-Opening Metathesis Polymerization of a Macrobicyclic Olefin Bearing a Sacrificial Silyloxiide Bridge. *Angew. Chemie. Int. Ed.* **2022**, *61* (2), e202112526.
23. Xu, Y.; Xu, W. L.; Smith, M. D.; Shimizu, L. S., Self-assembly and ring-opening metathesis polymerization of a bifunctional carbonate–stilbene macrocycle. *RSC Adv.* **2014**, *4* (4), 1675-1682.
24. Peng, Y.; Decatur, J.; Meier, M. A. R.; Gross, R. A., Ring-Opening Metathesis Polymerization of a Naturally Derived Macrocyclic Glycolipid. *Macromolecules* **2013**, *46* (9), 3293-3300.

25. Ibrahim, T.; Ritacco, A.; Nalley, D.; Emon, O. F.; Liang, Y.; Sun, H., Chemical recycling of polyolefins via ring-closing metathesis depolymerization. *Chem. Commun.* **2024**, *60* (11), 1361-1371.
26. Monfette, S.; Fogg, D. E., Equilibrium Ring-Closing Metathesis. *Chem. Rev.* **2009**, *109* (8), 3783-3816.
27. Garnes-Portolés, F.; Leyva-Pérez, A., Macrocyclization Reactions at High Concentration ($\geq 0.2\text{M}$): The Role of Catalysis. *ACS Catal.* **2023**, *13* (14), 9415-9426.
28. Foster, J. C.; Zheng, J.; Arifuzzaman, M.; Rahman, M. A.; Damron, J. T.; Guan, C.; Popovs, I.; Galan, N.; Demchuk, Z.; Saito, T., Closed-loop recycling of semi-aromatic polyesters upcycled from poly(ethylene terephthalate). *Cell. Rep. Phys. Sci.* **2023**, *4* (12), 101734.
29. Tracz, A.; Matczak, M.; Urbaniak, K.; Skowerski, K., Nitro-Grela-type complexes containing iodides – robust and selective catalysts for olefin metathesis under challenging conditions. *Beilstein J. Org. Chem.* **2015**, *11*, 1823-1832.
30. Nechmad, N. B.; Phatake, R.; Ivry, E.; Poater, A.; Lemcoff, N. G., Unprecedented Selectivity of Ruthenium Iodide Benzylidenes in Olefin Metathesis Reactions. *Angew. Chemie. Int. Ed.* **2020**, *59* (9), 3539-3543.
31. Kricheldorf, H. R., The Role of Self-Dilution in Step-Growth Polymerizations. *Macromol. Rapid. Commun.* **2008**, *29* (21), 1695-1704.
32. Kricheldorf, H. R.; Scheliga, F.; Weidner, S. M., What Does Conversion Mean in Polymer Science? *Macromol. Chem. Phys.* **2021**, *222* (8), 2100010.

33. Sytniczuk, A.; Dąbrowski, M.; Banach, Ł.; Urban, M.; Czarnocka-Śniadała, S.; Milewski, M.; Kajetanowicz, A.; Grela, K., At Long Last: Olefin Metathesis Macrocyclization at High Concentration. *J. Am. Chem. Soc.* **2018**, *140* (28), 8895-8901.
34. Kricheldorf, H., The Role of Cyclization and a New Theory of Polycondensation. In *Polycondensation: History and New Results*, Kricheldorf, H., Ed. Springer Berlin Heidelberg: Berlin, Heidelberg, 2014; pp 95-116.
35. Conrad, J. C.; Eelman, M. D.; Silva, J. A. D.; Monfette, S.; Parnas, H. H.; Snelgrove, J. L.; Fogg, D. E., Oligomers as Intermediates in Ring-Closing Metathesis. *J. Am. Chem. Soc.* **2007**, *129* (5), 1024-1025.